J Electr Eng Technol Vol. 9, No. 1: 143-153, 2014
http://dx.doi.org/10.5370/JEET.2014.9.1.143

ISSN(Print) 1975-0102
ISSN(Online) 2093-7423

Design and Implementation of Enhanced Resonant Converter for EV Fast Charger

Suk-Ho Ahn†, Ji-Woong Gong*, Sung-Roc Jang, Hong-Je Ryoo** and Duk-Heon Kim*****

Abstract – This paper presents a novel application of LCC resonant converter for 60kW EV fast charger and describes development of the high efficiency 60kW EV fast charger. The proposed converter has the advantage of improving the system efficiency especially at the rated load condition because it can reduce the conduction loss by improving the resonance current shape as well as the switching loss by increasing lossless snubber capacitance. Additionally, the simple gate driver circuit suitable for proposed topology is designed. Distinctive features of the proposed converter were analyzed depending on the operation modes and detail design procedure of the 10kW EV fast charger converter module using proposed converter topology were described. The proposed converter and the gate driver were identified through PSpice simulation. The 60kW EV fast charger which generates output voltage ranges from 50V to 500V and maximum 150A of output currents using six parallel operated 10kW converter modules were designed and implemented. Using 60kW fast charger, the charging experiments for three types of high-capacity batteries were performed which have a different charging voltage and current. From the simulation and experimental results, it is verified that the proposed converter topology can be effectively used as main converter topology for EV fast charger.

Keywords: Electrical engineering, Battery chargers, Converters, Resonant power conversion, DC-DC power conversion

1. Introduction

There has been great attention to eco-friendly electric vehicles due to concerns about environment and the regulation on emissions. Since middle 1990s, the advanced technology of Li-ion battery has accelerated the development of pure electric vehicles for commercialization by major automobile companies [1]. To promote the utilization of pure Electric Vehicles, however, there should be further enhancement in expanding distance of automobile running as well as in building infrastructure that provides the fast charging system, which enables a battery to be recharged up to 80% to 90% of the initial capacity [2-4]. The requirements of DC-DC converter adjustable to the fast charging system for Pure Electric Vehicles are as follows:

- The high capacity of charging current which does not affect the life-cycle of a battery.
- The high efficiency in the rated operating condition.
- The high quality of constant current regulation, which allow a battery to be charged safely and rapidly.
- The wide range of output voltage for charging batteries with diverse capacity.

Especially, compared to an on-board charger, a fast charging converter is operated under rated load since an off-board fast charging system requires the maximum charging current of a battery to be constant. Therefore, the use of the fast charging converter under the light load area is limited, and it is important to increase the efficiency at rated current. According to the aforementioned requirements, SRC(series loaded resonant converter) could be applied for the fast charging converter, which can operate as a current source and make it possible to achieve the high efficiency by reducing switching loss. But below resonance operating DCM(Discontinuous Conduction Mode) SRC has the disadvantages of audible noises depending on load conditions and high conduction loss as a high crest factor while it enables both turn on and turn off to soft switch [5-6]. Furthermore, above resonance operating CCM (Continuous Conduction Mode) SRC has disadvantages that light load loss increases, as switching frequency increases during light load and the turn off loss is existed. In order to overcome this weakness, lossless snubber capacitor, for reducing a turn off loss, can be employed although it is limited to increase of capacitance. On the other hand, it has a relatively lower conduction loss and a high efficiency at rated current [7-9]. It can be the most effective alternative in the field that mostly operated in rated load range, restricted to using it in a light load range like the fast charger. In addition, among resonant converters,

† Corresponding Author: Dept. of Energy Conversion, University of Science & Technology, Korea. (whiteyan@keri.re.kr)
* Dept. of Energy Conversion, University of Science & Technology, Korea. (smarty0@keri.re.kr)
** Electric Propulsion Center, Korea Electro-technology Research Institute, Korea. ({scion10, hjryoo}@keri.re.kr)
*** Dept. of Electric Railway, Catholic Sang-ji College, Korea. (dhkim @csj.ac.kr)
Received: March 4, 2013; Accepted: July 6, 2013

the LLC Resonant Converter, such as the power supply for LCD TV or Plasma Display Panel, is characterized by high efficiency operating under constant load. Despite the wide use of this resonant converter, it has drawbacks such as difficulty in designing a transformer and the limited capacity due to magnetizing current that generates heat. For designing it as a universal charger with wide range of output voltage, the LLC resonant converter with big voltage gains should be applied. For this reason, a transformer with a low magnetizing inductance value should be used for configuring the system, and that leads to the increase conduction loss and current stress by increasing transformer's magnetizing current. Besides, there is a limit in changing it into a large capacity of kW class due to the difficulty in designing the transformer and heat generation of transformer [10-11].

In this paper, LCC-SRC, which has been developed as the DC-DC Converter for electric vehicle fast chargers, as well as the new gate driver circuit adapting to the proposed converter will be proposed. The LCC-SRC, which is a switching converter operating with above resonant frequency, consists of lossless snubber capacitor with relatively high capacitance and the combination of secondary winding and supplementary capacitor. Because of the supplementary capacitor, it can reduce the rising time of the resonant current, improves a resonant current waveform to reduce conduction loss. The converter makes it possible effectively increasing the lossless snubber capacitance. Therefore, compared to the CCM SRC, the proposed converter can maximize the efficiency under rated current by decreasing turn off loss and conduction loss. The converter maintains SRC converter's current source operating characteristics by adding a low value of the supplementary capacitor, which in turn facilitates the converter's parallel operation, easily expands the capacity of the electric vehicle fast charger, and stabilizes the design of the system with redundancy. In addition, the gate driver circuit for the converter is aimed at having appropriate variable dead time and accurate zero voltage detection is embodied in the converter. In order to verify the validity, this paper deals with the basic operation and features of the proposed converter with a new gate driver circuit. The optimized design for the 60kW fast charger, composed of six 10kW converter modules is described. The advantages of the converter are proved through various simulation and actual load experiments as well.

2. Analysis of Proposed Resonant Converter Topology

The LCC-SRC for the EV fast charger, as the Fig. 1. illustrates, consists of the full bridge inverter for high frequency switching, the snubber capacitor (C_1~C_4) for reducing turn off loss, the resonant tank (C_r, L_r) in series with the load, the parallel resonant capacitor (C_s) for reducing the loss of the switching device, the rectifier

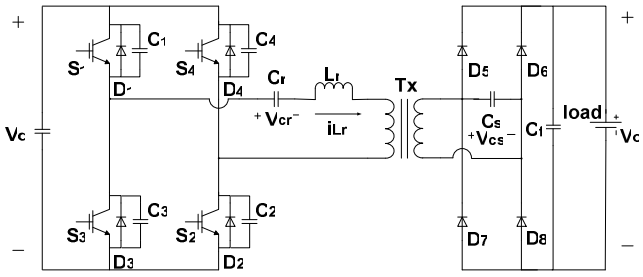

Fig. 1. Scheme of enhanced series loaded resonant converter

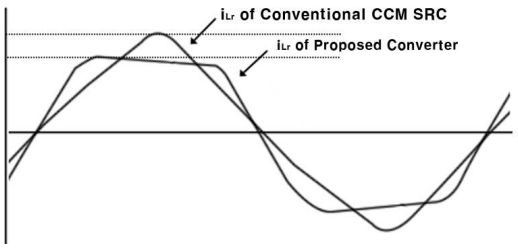

Fig. 2. Comparison of resonant waveform between conventional CCM SRC and proposed converter under the same RMS output

(D_5~D_8), and the output filter capacitor (C_f). While the proposed converter has the same formation as the conventional LCC type resonant converter, which has a lossless snubber, the parallel resonant capacitor of the transformer secondary winding, compared to the series resonant capacitor of the transformer primary winding, has relatively very low value in order to gain fast rising time of the current through the resonant tank circuit.

The advantages of LCC-SRC include reduction of switching loss and conducting loss, the possibility of mass capacity with a form of module combination, and increase of power density. Therefore, if the proposed converter is applied to an EV fast charger, it can be possible to achieve high efficiency under rated load. If the proposed converter is operated under the higher switching frequency than resonance frequency the turn on loss will be reduced due to possibility of ZVZCS (Zero Voltage Zero Current Switching). Furthermore, although the very small amount of the parallel resonant capacitor cannot make modification in the current source attributes of the conventional SRC, it can transform the waveform of resonant current from the existing sinusoidal waveform to the trapezoidal formation as shown in Fig. 2. If the resonant current of the trapezoidal formation is rectified, the ripple of load current will be significantly reduced compared to the conventional CCM SRC, and the conducting loss will be decreased by enhancing the crest factors. Also, by increasing the energy accumulated in the resonant inductor, the rapidly rising resonant current can discharge the energy accumulated in the snubber capacitor. This enables the relatively large amount of the lossless snubber capacitor to be applied to the converter, effectively reducing the turn off loss.

To analyze the steady state and the mode of the suggested

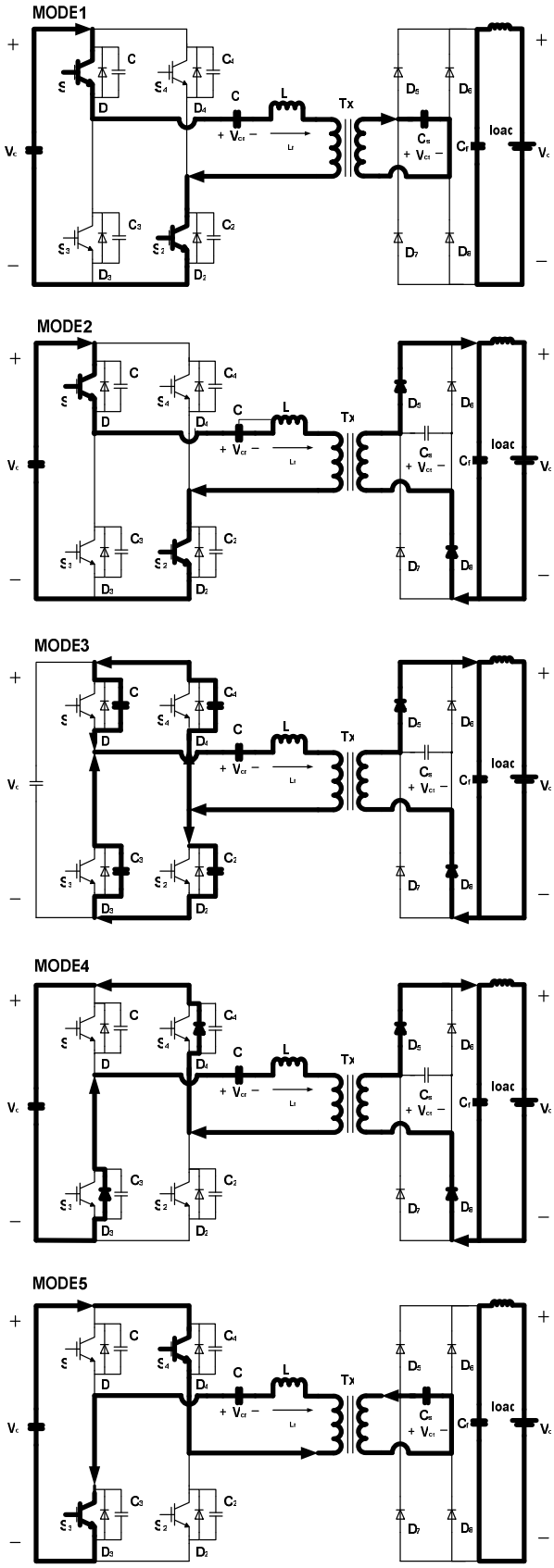

Fig. 3. Operation mode diagrams of proposed converter

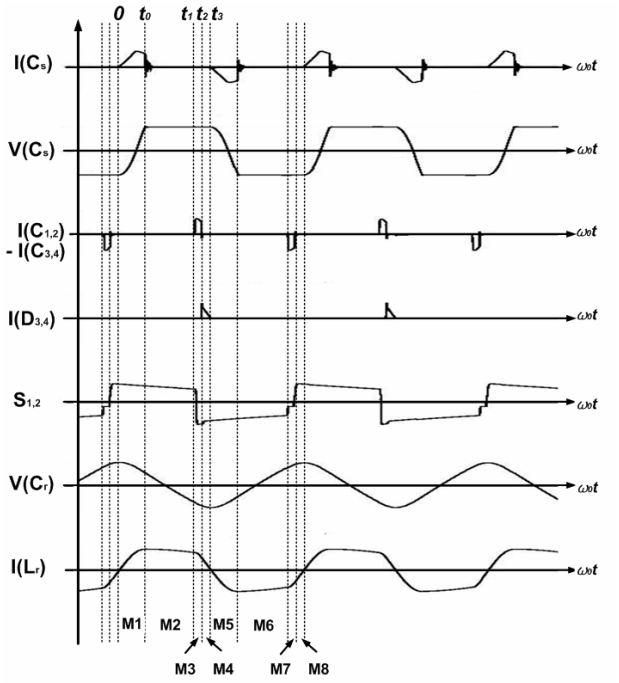

Fig. 4. Operation waveforms of proposed converter

converter, there are assumptions as follows

- The forward voltage drop and the on state resistance of the switching element used in the converter are ignored.
- The parasitic elements of the capacitor and the inductor are ignored.
- The input voltage (Vd) is assumed to be DC voltage, which has no ripple elements.
- The value of the output capacitor (Cf) is very large, and the output voltage from each mode is DC voltage.

Under the Steady state, the proposed converter can be divided into 8 modes within each operating cycle. And the operation circuit diagram and the operation waveform based upon each mode are shown as the Figs. 3 and the Fig. 4. respectively, and the analysis of each steady state and principle of operation are discussed as follows.

MODE 1 (M1, $0 \le t < t_0$): Before the beginning of this mode (t=0), the parallel resonant capacitor (C_s) is charged with $-V_0$, and the switch S_1 and S_2 is under the condition of the ZVZC turn on. MODE 1 begins when the input voltage (V_d) is exposed to the resonance tank by changing the direction of the resonant inductor current (i_{Lr}). Under this mode, the resonant current (i_{Lr}) through the resonance tank charges the parallel resonant capacitor (C_s). This mode ends when the charged voltage (V_{cs}) increases to the output voltage (V_o). At this point, regardless of load, the rising resonant current (I_{Lr}) can be shown as the following Eq. 1.

$$i_{Lr}(t) = I_{Lr0}\cos\sqrt{2}\omega_0' t + \frac{(V_d - V_{cr0} - V_{cs0})\sin\sqrt{2}\omega_0' t}{\sqrt{2}Z_0'} \qquad (1)$$

Where, $i_{Lr}(0)=I_{L0}$, $V_{cr}(0)=V_{cr0}$, $V_{cs}(0)=V_{cs0}=-NV_o$, $Z_o'=\sqrt{\frac{L_r}{C_r'}}$ $\omega_0'=\frac{1}{2\pi\sqrt{L_rC_r'}}$, $C_r'=\frac{a^2C_rC_s}{C_r+a^2C_s}$, $a=\frac{N_2}{N_1}$

In this mode, the voltages across the series and the parallel resonant capacitor are shown in the time domain as the followings.

$$V_{cr}(t)=\frac{1}{2}\begin{bmatrix}(V_d+V_{cr0}+V_{cs0})-(V_d-V_{cr0}-V_{cs0})\cos\sqrt{2}\omega_0't\\+\sqrt{2}Z_0'I_{L0}\sin\sqrt{2}\omega_0't\end{bmatrix} \quad (2)$$

$$V_{cs}(t)=\frac{1}{2}\begin{bmatrix}(V_d+V_{cr0}+V_{cs0})-(V_d-V_{cr0}-V_{cs0})\cos\sqrt{2}\omega_0't\\+\sqrt{2}Z_0'I_{L0}\sin\sqrt{2}\omega_0't\end{bmatrix} \quad (3)$$

MODE 2 (M2, $t_0 \le t < t_1$): In this range, the parallel capacitor voltage (V_{cs}) is clamped to the DC output voltages ($V_{cs}=V_o$), and does not contribute to the converter's resonance phenomena. At this point, resonance current is delivered to load, and is gradually reduced by the output voltage as shown in the following Eq. 4.

$$i_{Lr}(t)=I_{L1}\cos\omega_0t+\frac{(V_d-V_o/a-V_{cr1})\sin\omega_0t}{\sqrt{2}Z_0} \quad (4)$$

Where, $i_{Lr}(t_0)=I_{L1}$, $V_{cr}(t_0)=V_{cr1}$, $Z_o=\sqrt{\frac{L_r}{C_r}}$, $\omega_0=\frac{1}{2\pi\sqrt{L_rC_r}}$

In this process, the voltage of the series resonant capacitor voltage can be gained as follows.

$$V_{cr}(t)=(V_d-V_o/a)-(V_d-V_o/a-V_{cr1})\cos\omega_0t+Z_0I_{L1}\sin\omega_0t \quad (5)$$

MODE 3 (M3, $t_1 \le t < t_2$): By the control signal, the switch S_1 and S_2 is turned off, and then resonance current by the energy accumulated in the resonance tank charges C_1 and C_2, discharging C_3 and C_4 with freewheeling.

This time, the voltage across the switches gradually increases as shown in the following Eq. 6.

$$V_{CE}=\frac{1}{C_{1\sim4}}\int_{t1}^{t2}i_{C1\sim4}dt=\frac{1}{C_{1\sim4}}\cdot\frac{ILr}{2}t_{M3} \quad (6)$$

Where, $i_{C1\sim4}=\frac{ILr}{2}$

In this mode, unless the lossless snubber capacitor is completely discharged, the turn on loss occurs in the subsequent switching period. Thus, MODE 3 should be maintained in order for the lossless snubber capacitor to be completely discharged, The time period is calculated by using the following Eq. 7.

$$t_{M3}=t_{DT(\min)}=\frac{2V_d\cdot C_{1\sim4}}{I_{Lr}} \quad (7)$$

If the lossless snubber capacitor has quite a large value, the voltage across the switch in the turn off period approaches to zero, and the turn off loss of the switch is reduced.

In this mode, resonance current as shown in the Eq. 8. is delivered to load, gradually reducing. After this, the series resonant capacitor voltage is calculated by the following Eq. 9.

$$i_{Lr}(t)=\frac{1}{2B}e^{At}\begin{bmatrix}(e^{-2At}+1)BI_{Lr2}\\-C_rC_{1,2}(e^{-2At}-1)(V_{cr2}+V_d-V_o/a)\end{bmatrix} \quad (8)$$

$$V_{cr}(t)=\frac{1}{C_r(C_r-C_{1,2})}\begin{bmatrix}C_r(C_rV_{cr2}+C_{1,2}V_d-C_{1,2}V_o/a)\\-C_rC_{1\sim4}(V_{cr2}+V_d-V_o/a)\cosh At\\-I_{L2}B\sinh At\end{bmatrix} \quad (9)$$

Where, $A=\frac{(C_{1,2}-C_r)}{\sqrt{C_{1,2}(C_r-C_{1,2})C_rL_r}}$, $B=C_{1,2}(C_r-C_{1,2})C_rL_r$, $i_{Lr}(t_1)=I_{Lr2}$, $V_{cr}(t_1)=V_{cr2}$

MODE 4 (M4, $t_2 \le t < t_3$): Once the lossless snubber capacitor C_1 and C_2 are fully charged, resonance current flows through body diode D_3 and D_4. The voltage and the current across the switch S_3 and S_4 are almost zero, possible for S_3 and S_4 to ZVZC turn on. The resonance current and the series resonant capacitor voltage are the following Eq. 10. and 11.

$$i_{Lr}(t)=I_{Lr3}\cos\omega_0t-\frac{(V_O/a+V_{cr3})\sin\omega_0t}{Z_0} \quad (10)$$

$$V_{cr}(t)=-V_o/a+(V_{cr3}+V_o/a)\cos\omega_0t+Z_0I_{Lr3}\sin\omega_0t \quad (11)$$

Where, $i_{Lr}(t_2)=I_{Lr3}$, $V_{cr}(t_2)=V_{cr3}$, $a=\frac{N_2}{N_1}$

There is the same analysis for MODE 5 to MODE 8, the equation can be elicited by the aforementioned procedure.

3. Design of the Proposed Converter for EV Fast Charger

To examine whether the proposed converter appropriate for EV fast charger, designing EV fast charger with the high efficiency of 60kW rating is encouraged. The intended

EV fast charger enables charging voltage to change from 50V to 500V so that a variety of batteries aimed at full speed EV and NEV (Neighborhood Electric Vehicle) can be charged up to SOC (State of Charge) 80% within 30 minutes. In this section, the considerations for designing the proposed converter with the highly effective EV fast charger, and the proposal of PSpice model for the validity of designing the proposed converter will be discussed. Fig. 5. illustrates the whole structure of 60kW EV fast charger, comprised of circuit breaker, the soft start part to prevent inrush current, rectifying section, the PFC part for power factor correction and reducing the ripple of DC voltage, the converter module part which connects the six proposed 10kW converter in parallel, and the control part for stable output and converter protection

The design rules for proposed converter can be summarized as follows.

1) The EV Fast Charger is mostly operated at rated charging current to reduce the charging time. Therefore, the efficiency at rated operation is the most important thumb of design rules for designing the proposed converter.
2) For the battery charging, both of charging current control and charging voltage control should be considered. The converter topology such as series-parallel resonant converter which has both voltage and current source characteristics is suitable for the EV Fast Charger.
3) The EV Fast Charger should be operated for charging various types of batteries which were installed at various EV with different charging voltage. From the above reason, it is needed for converter design to consider the wide range of output voltage for various kinds of EV battery charging.

3.1 Design of 10kW LCC-SRC

The procedures for designing the parameter of the 10kW proposed converter are as follows. First, depending on frequency tolerance of switching elements, switching frequency is determined, and then resonance frequency is decided. After that, based on the energy accumulated in the resonant inductor, the value of parallel resonant capacitor is chosen and the value of series resonant capacitor and resonant inductor is calculated. Finally, through the parameter that is determined in the previous procedure, the value of lossless snubber capacitor is decided. The following is under consideration of designing.

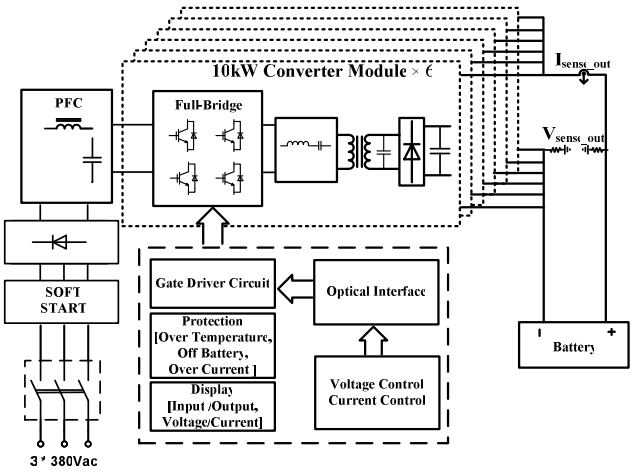

Fig. 5. Overall structure of 60kW EV fast charger

Switching Frequency and Resonant Frequency: To avoid audible noise, the minimum of switching frequency should be beyond the range of audio frequency, and the maximum of switching frequency should not exceed the maximum frequency tolerance of switching device as well as the frequency of the converter's minimum operating point. Since the proposed converter operates in the range of CCM, resonance frequency should be decided below the range of switching frequency, and the range of switching frequency should be designed to operate within the linear interval of character impedance so that the control of output voltage can be facilitated.

Parallel Resonant Capacitor: To reduce conduction loss with enhanced Crest factors, parallel resonant capacitor should be designed with the value as small as possible. However, due to decreasing parallel resonant capacitor, flowing current of resonant inductor decreases, and in turn energy stored in the inductor is decreased. In this way, since it is impossible to discharge lossless snubber capacitor, the conditions of ZVZCS cannot be met. Therefore, the value of parallel resonant capacitor should be minimized within the ZVZCS range.

To determine the optimal value of parallel resonance capacitor, Fig. 6(a). is the waveform of resonance current simulation that analyzes a variety of values by changing the value of parallel capacitor for the proposed converter based on the criteria of the conventional CCM SRC. Each comparative converter is designed to equalize the output condition (500V 20A) and turn-off loss to each other. Fig. 6(b). is the waveform that compares each converter's conduction loss, showing that conduction loss is decreased as the value of parallel resonant capacitor decreases.

From the simulated IGBT loss comparison depicted in Fig.6.(b), it is clear that the proposed converter has less loss compared to the conventional resonant converter. Also, the efficiency of the proposed converter was measured as 98.5%. Compare to 96.5% of the conventional CCM SRC which was designed to have maximum efficiency at rated operation, the advantage of the proposed converter was verified and the strength of the proposed converter as the EV Fast Charger was confirmed. However, it should be noted that the proposed converter has less efficiency at light load condition due to the relative circulating energy.

Series Resonant tank: Once parallel resonant capacitor is determined, series resonant capacitor should be designed not to change the characteristics of SRC current source.

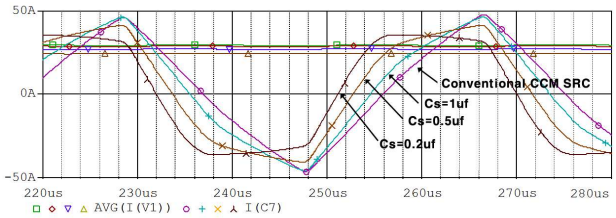

(a) Resonant current (Time : 2us/div. Resonant Current, 50A/div.)

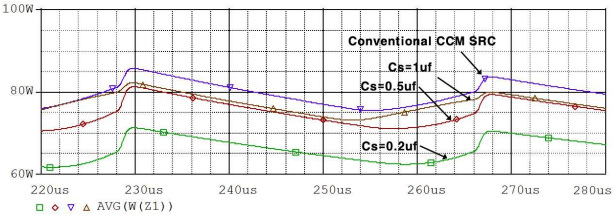

(b) Switch loss (Time : 2us/div. Switch loss, 5W/div.)

Fig. 6. Comparison of waveform based on the parallel resonant capacitor changes

The value of series resonant capacitor should be designed 10 to 15 times more than the value of parallel resonant capacitor. After deciding the value of resonance frequency, character impedance, and series and parallel resonance capacitor, the value of resonant inductor can be calculated. At this point, the value of character impedance is calculated based on the capacity of the converter and the maximum value of load current.

Lossless snubber capacitor: The value of lossless snubber capacitor should be designed as the maximum value that allows lossless snubber capacitor to be fully discharged within the freewheeling time of resonant current after switch is turned off. Fig. 7. compares switching loss by changing the value of lossless snubber capacitor from the maximum value for the conventional CCM SRC with the same output condition to the maximum value for the proposed converter. In Fig. 7, turn off loss can be decreased to almost zero.

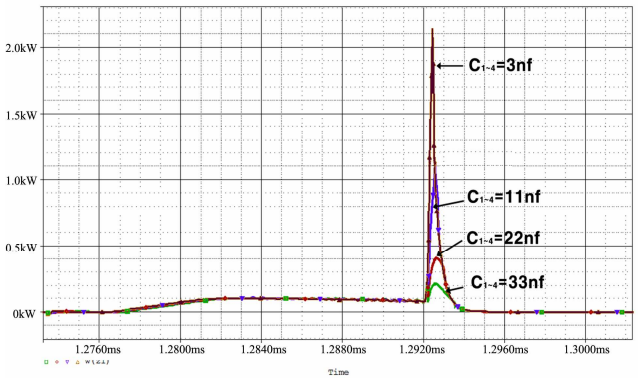

Fig. 7. Comparison of switch loss based on the lossless snubber capacitor changes (Time : 1us/div. Switch loss, 0.1W/div.)

3.2 Design of the gate driver circuit for proposed converter

The conventional gate driver that has fixed dead time is difficult to apply to the proposed converter because the proposed converter operates with soft switching within wide load range. This paper proposes the gate driver that has variable dead time and simple structures by detecting the voltage across switching devices and determining when to turn on. The proposed gate driver does not need two opposite control signal with dead time, while it uses a single control signal with half duty that only has operating frequency. As the control signal is simplified, it facilitates the use of a transformer for isolation and photoelectric elements, having a competitive advantage in digitalization. To analyze the operating principle of the proposed gate driver, four different modes will be explained as shown in Fig. 8. In case of the gate driver circuit which has variable dead time for detecting zero voltage, there is a problem in which the main switch fails to turn on since the voltage across main switches does not meet the condition of zero voltage under light loading or at soft start. To solve this problem, the normal operation of the converter should be guaranteed by setting the maximum dead time and forcefully turning on, even if this could not fulfill the requirement for zero voltage on time. In the Dead Time Mode, when turn on control signal is applied in the input of the gate driver circuit, capacitor C_1 starts to be charged while the main switch does not turn on because current flows through C_1, R_1, and R_4 (more resistance compared to R2) of the secondary transformer. If the electric potential of the main switch IGBT Collector-Emitter approaches zero before C_1 voltage being charged to V_{th}(turn on threshold Voltage of P-Channel MOSFET), current flows through C_1, R_1, R_2 (less resistance compared to R_4), and the voltage of capacitor C1 is rapidly charged up to V_{th}, turning on the main switch as Zero Voltage Detection Mode in Fig. 9. Finally, if the zero voltage condition is met before the determined maximum dead time ends, the main switch turns on in operation. During C_1 is being charged in Dead Time Mode, although zero voltage is not detected, the charging voltage of C_1 becomes V_{th}. At this time, the

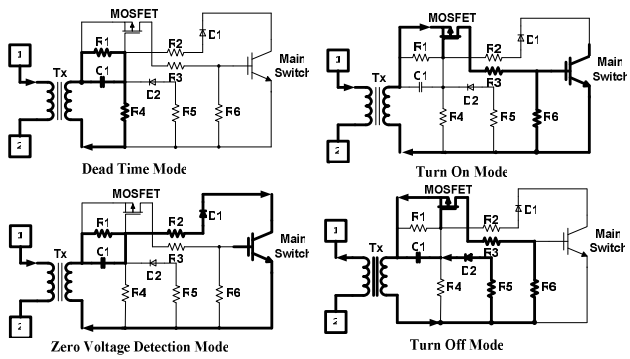

Fig. 8. Mode analysis of proposed gate driver circuit

current of the gate driver circuit turns on IGBT, the element of the main switch, through MOSFET and R_3. Capacitor C_1 can set the time of being charged to V_{th} as the maximum dead time of the main switch (IGBT), determining the value of the gate driver circuit R_1, R_4, and C_1 to meet the following equation.

$$t_{DT(\min)} = \frac{2V_d \cdot C_{1\sim4}}{I_{Lr}} < -\frac{R_1 R_4 C_1}{R_1 + R_4} \ln(1 - \frac{V_{th}}{V_{in}}) \qquad (12)$$

Where, V_{th} : Gate-source turn on voltage of MOSFET, V_{in} : Gate-driver input voltage

In the Turn Off Mode, the turn off control signal is applied in the gate driver input in order to turn off the main switch. In turn, current flows through R_6 of the secondary transformer and the body diode of MOSFET, and the main switch turns off. Also, the current flowing through R_5 and D2 discharges C_1, resetting the Dead Time Mode operation for the next period.

3.3 Simulation of proposed converter

To identify the operation of the proposed converter and the validity of designing the proposed converter, the simulation for 10kW enhanced CCM SRC using PSpice was performed. The converter used for the simulation was designed by the procedures mentioned before, and the parameter of the designed converter is shown as Tab.1. The utilized PSpice model was simulated under consideration of the forward voltage drop and on-state resistance of the switch and the diode device, saturation and loss of the transformer for the converter circuit including the proposed gate drive as shown in Fig. 9. Fig. 10(a). is the waveform of output voltage, output current, resonant current and switching signal under 10kW maximum output with 400V, 25A condition, which the validity of the designed converter parameter can be analyzed. In this figure, the waveform of resonant current in rated current, as discussed earlier, has a trapezoidal form, which significantly reduces conduction loss. Fig. 10(b). is the waveform showing switching device current and voltage, and meeting turn on ZVZCS condition.

Table 1. Summary of Design Parameters for the 10kW Converter Module

Design Parameters	
DC Link Voltage, V_d	513Vdc±10%
Output Voltage, V_o	0~500V
Output Current, I_o	0~25A
Output Power, P_o	10kW
Resonant Inductance, L_r	115uH
Resonant Capacitance, C_r	3uF
Second Resonant Capacitance, C_s	0.204uF
Transformer Turn Ratio, N	17:14
Switching Frequency, fs	24kHz-77kHz
Snubber Capacitance, C_1~C_4	33nF

Also, turn off loss becomes almost zero influenced by the lossless snubber capacitor. Fig. 11. shows the change of output current depending on switching frequency in order to analyze the converter's control performance under different loading conditions. As shown in Fig. 11., where the relation between output current and switching frequency is linear, controlling the output of the converter is facilitated.

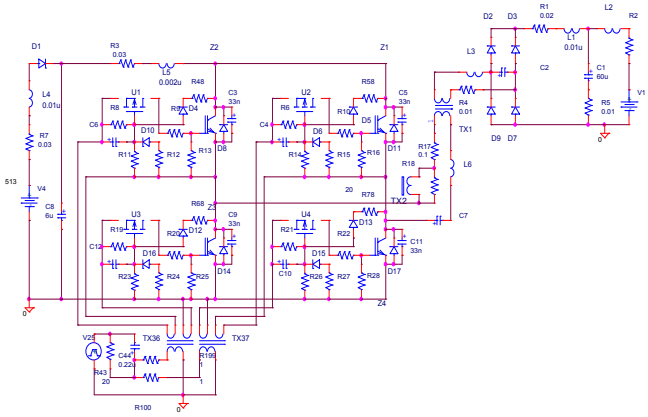

Fig. 9. PSpice model of proposed 10kW converter module

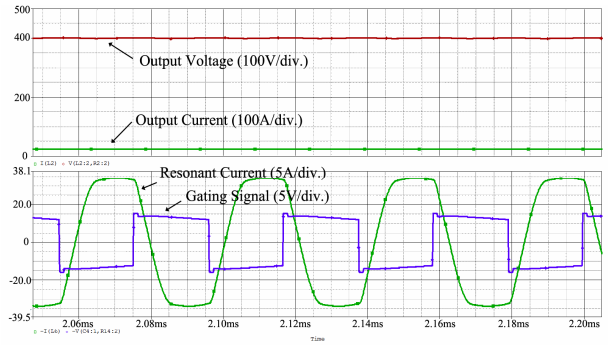

(a) Output voltage, output current, resonant current and gating signal (Time : 5us/div.)

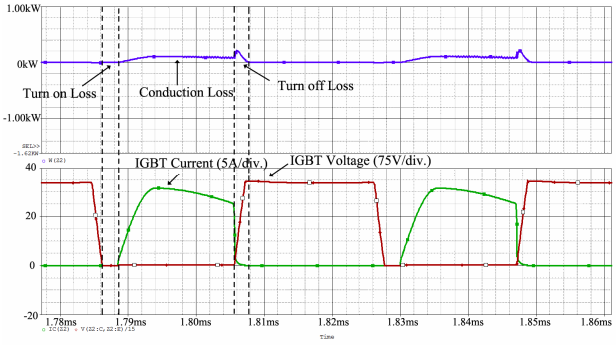

(b) Loss analysis of IGBT device (Time : 2us/div. Loss : 200W/div.)

Fig. 10. Simulation results of 10kW proposed converter module

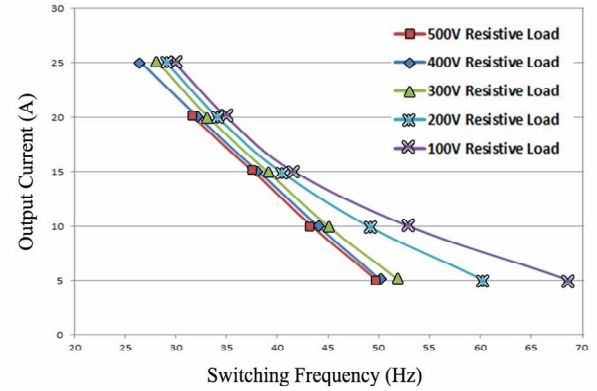

Fig. 11. Simulation result of output current vs. switching frequency for load change

Fig. 12. Picture of 20kW converter block consisted of two 10kW modules

(a) Charging test setup for 320V 20kWh LiFePO4

(b) Test setup for battery charging simulator

Fig. 13. Experiment setup for 60kW fast charger

Table 2. Specification of 20kW Converter Block

Size(mm) (W,H,D)	480×180×270 (23.4 ℓ)
Output	10kW (400V-25A, 500V-20A)
Maximum Efficiency	98.5%
Power Density	1.17 ℓ/kW

4. Experimental Results

Applying the converter design parameter examined through the simulation, 60kW EV Fast Charger was implemented with six 10kW converter modules. Tab. 2. and Fig. 12. are the specification and the actual outer shape of 20kW block comprised of two 10kW converter modules. Fig. 13(a). is the experiment scene in which 320V 20kWh LiFePo4 battery is charged with 60kW EV Fast Charger that was implemented with three 20kW converter blocks in parallel. Fig. 13(b). is the experimental setup with variable resistive load for simulating the battery of 400V and 500V condition. To test the operation character and performance, experiments for maximum output, output variation, actual loading, and efficiency measure were performed with regard to 10kW converter module and 60kW fast charger by utilizing simulated test resistive load and a various kinds of batteries. Fig. 14. is the experiment waveform that shows output voltage, output current, resonant current, and switching signal when 10kW converter modules operate in the maximum rated output. The efficiency was measured as 98.5%, and as shown in Fig. 15. The high efficiency was maintained under various output conditions. To prove that it is possible to install the massive capacity EV fast charger in the form of parallel combination of the converter module,

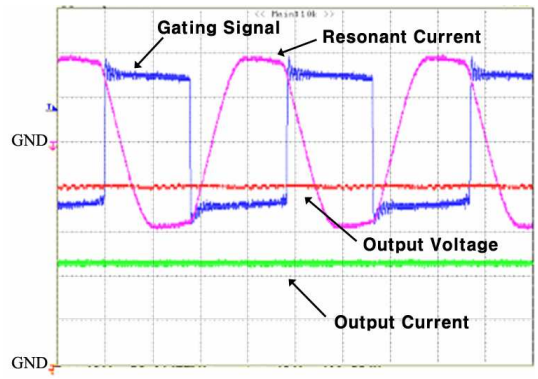

Fig. 14. Experimental results of 10kW converter module (Time scale: 10us/div. Gating Signal, 10V/div. Resonant Current, 20A/div. Output Voltage, 100V/ div. Output Current, 20A/div.)

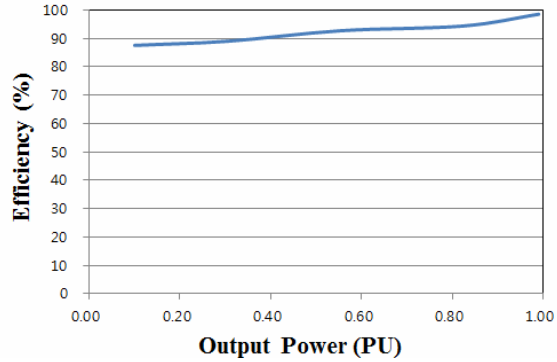

Fig. 15. Efficiency measurement depending on the load

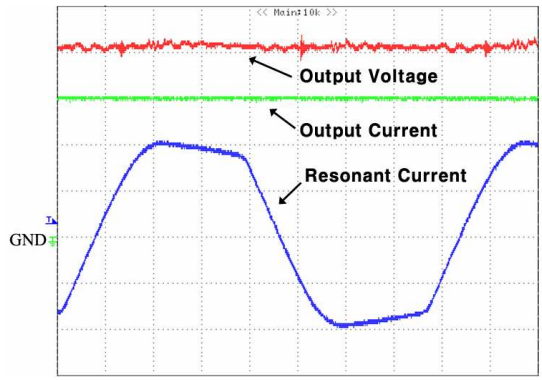

(a) Output voltage : 400V

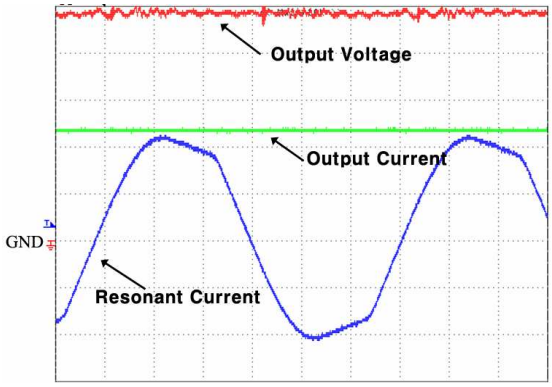

(b) Output voltage : 500V

Fig. 16. Experimental results of 60kW EV fast charger (Time Scale: 5us/div. Resonant Current, 20A/div. Output Current, 50A/div. Output Voltage, 100V/div)

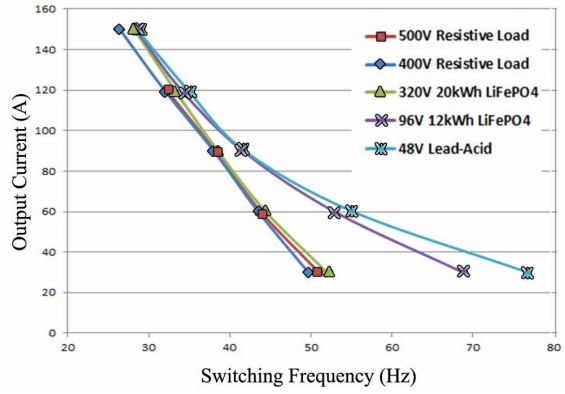

Fig. 17. Experiment result of output current vs. switching frequency for load change for different load

six converter modules connected in parallel with 60kW fast charger were experimented. Fig. 16 is the experiment waveform that confirms steady state operation under 60kW maximum output when it comes to output voltage, output current, and resonant current. At that time, measured maximum efficiency was 97% under the condition of 454V, 139A. The experiment result of charging current depending on the variation of switching frequency under various

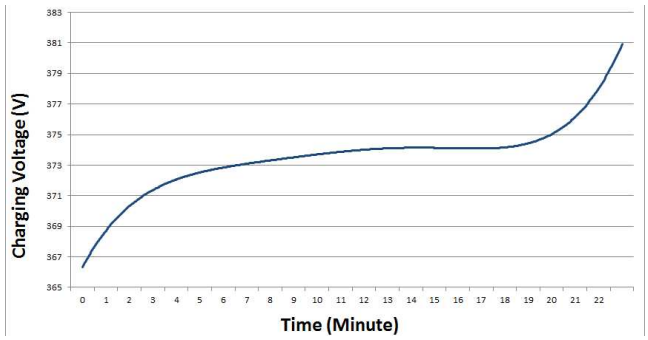

(a) Voltage plot for charging time measurement

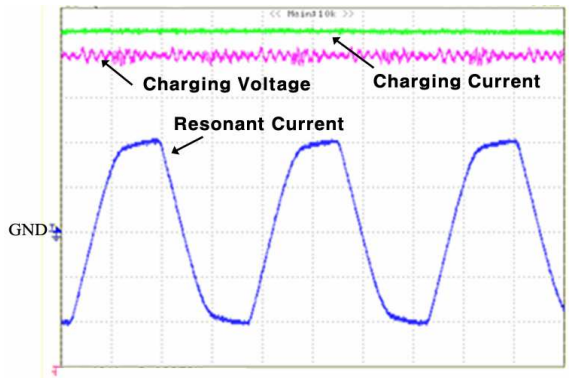

(b) Detail waveforms of 60kW fast charger (Time : 10us/ div. Resonant Current, 20A/div. Charging Voltage, 50V/ div. Charging Current, 20A/div.)

Fig. 18. Experimental results for 320V 60Ah LiFePO2 charging test

kinds of load condition in order to verity its performance with real battery charging condition is shown as Fig. 17. When it operates with 48V, 3.8kWh Lead-Acid, 96V 12kWh LiFePO4 battery, 320V 19.2kWh LiFePO4 battery, and variable resistive load for simulating higher voltage battery charging condition of 400V and 500V, the experiment was performed to test the common use of fast chargers varying from output charging voltage of 50V to 500V. Currently used for the full speed EV, 320V and 19.2kWh LiFePO4 batteries were experimented to measure charging time and charging function. Fig. 18(a). shows charging voltage based on charging time. As Fig. 18(a). shows, the charging time from SOC 10% to 90% was about 17 minutes, valid for the EV fast charger. The waveform of the resonant current, the charging voltage, and the charging current are shown in Fig. 18(b).

5. Conclusion

In this paper, the enhanced converter topology based on series loaded resonant converter was proposed for EV fast charger. Adding small parallel resonant capacitor at output rectifier circuits and increasing the lossless snubber capacitance, the proposed converter has the advantage of

enhancing the system efficiency especially at the rated load condition because it can reduce the conduction loss by improving the resonance current shape and minimize turn off losses. The design and implementation of the proposed converter have been described and distinctive features of the proposed converter were analyzed. Also, the simple gate drive circuit which can minimize the turn on loss by active detecting zero voltage condition of the IGBT was developed for the proposed converter. The 60kW EV fast charger having an output voltage range of 50V~500V was developed using proposed converter topology and various kinds of test were performed to verify that the proposed resonant converter is suitable for EV Fast charger. The basic tests of the developed EV fast charger were performed using resistive load bank which can simulate the various types of battery with different charging conditions. And real battery charging tests also performed by using three kinds different type of high capacity batteries. From the experiments, maximum efficiency was measured as 98.5% for 10kW DC-DC module, and 97% for a 60kw AC to DC EV fast charger including rectifying circuits. For the fast charging of 320V, 19.2kWh LiFePO4 battery, the charging time from 10% to 90% SOC was measured as 17 minutes. It was verified from various kinds of tests that proposed converter is suitable for the high efficiency EV fast charger which is usually operated at maximum rated charging current condition.

The developed EV fast charger was installed at Korean EV test infrastructure and practical charging test with various kinds of EVs has been now performing.

References

[1] Mahesh Kulkarni, “Mahindra Reva to launch five electric cars”, business Standard, September 13, 2012.

[2] Kutkut, N.H.; Divan, D.M.; Novotny, D.W.; Marion, R.H.; “Design considerations and topology selection for a 120-kW IGBT converter for EV fast charging,” Power Electronics, IEEE Transactions on, vol. 13, no. 1, pp.169-178, Jan 1998

[3] Klontz, K.W.; Esser, A.; Wolfs, P.J.; Divan, D.M.;, “Converter selection for electric vehicle charger systems with a high-frequency high-power link,” Power Electronics Specialists Conference, 1993. PESC '93 Record., 24th Annual IEEE, vol, no., pp. 855-861, 20-24 Jun 1993

[4] Kobayashi, Y.; Kiyama, N.; Aoshima, H.; Kashiyama, M.;, “A route search method for electric vehicles in consideration of range and locations of charging stations,” Intelligent Vehicles Symposium (IV), 2011 IEEE, vol, no., pp.920-925, 5-9 June 2011

[5] Shah, S.; Upadhyay, A.K.;, “Analysis and design of a half-bridge series-parallel resonant converter operating in discontinuous conduction mode,” Applied Power Electronics Conference and Exposition, 1990. APEC '90, Conference Proceedings 1990., Fifth Annual, vol, no., pp.165-174, 11-16 March 1990

[6] Belaguli, V.; Bhat, A.K.S.;, “Series-parallel resonant converter operating in discontinuous current mode. Analysis, design, simulation, and experimental results,” Circuits and Systems I: Fundamental Theory and Applications, IEEE Transactions on, vol.47, no.4, pp.433-442, Apr 2000

[7] R.L. Steigerwald, “A comparison of Half-bridge resonant converter topologies,” IEEE Trans. Power Electron., vol3, pp. 174-182, April 1988.

[8] Sloan, T.H.;, “Design of high-efficiency series-resonant converters above resonance,” Aerospace and Electronic Systems, IEEE Transactions on, vol.26, no.2, pp.393-402, Mar 1990 doi: 10.1109/7.53446.

[9] Sloan, T.H.;, “Design of high-efficiency series-resonant converters above resonance,” Aerospace and Electronic Systems, IEEE Transactions on, vol.26, no. 2, pp.393-402, Mar 1990.

[10] Beiranvand, R.; Rashidian, B.; Zolghadri, M.R.; Alavi, S.M.H.;, “Using LLC Resonant Converter for Designing Wide-Range Voltage Source,” Industrial Electronics, IEEE Transactions on, vol.58, no.5, pp. 1746-1756, May 2011

[11] Bong-Gun Chung; Kwang-Ho Yoon; Phum, S.; Eun-Soo Kim; Jong-Seob Won;, “A novel LLC resonant converter for wide input voltage and load range,” Power Electronics and ECCE Asia (ICPE & ECCE), 2011 IEEE 8th International Conference on, vol, no., pp. 2825-2830, May 30 2011-June 3 2011

Suk-Ho Ahn received the B.S. degree in electrical engineering from Incheon National University, Incheon, Republic of Korea, in 2009 and is currently pursuing both his M.S. and Ph.D. degrees at the University of Science & Technology (UST) in Daejeon, Republic of Korea. His research interests include the soft switched resonant converter applications and battery charger systems.

Ji-woong Gong received the B.S. in electrical engineering from Chonnam National University, Gwangju, Republic of Korea, in 2012 and is currently pursuing the M.S. degree at the University of Science & Technology (UST) in Daejeon, Republic of Korea. His research interests include the soft switched resonant converter applications and High Voltage Pulsed Power Supply Systems.

Sung-Roc Jang was born in Daegu, Korea, in 1983. He received his B.S. from Kyungpook National University, Daegu, Korea, in 2008, and the M.S. and Ph.D. in Electronic Engineering from the University of Science & Technology (UST), Deajeon, Korea, in 2011. Since 2011, he has been with the Korea Electro-technology Research Institute as a senior researcher of electric propulsion research center. His current research interests include high-voltage resonant converters and solid-state pulsed power modulators and their industrial applications.

Dr. Jang received the Young Scientist Award at 3rd Euro-Asian Pulsed Power Conference in 2010, and the IEEE Nuclear Plasma Science Society (NPSS) Best Student Paper Award at IEEE International Pulsed Power Conference in 2011.

Hong-Je Ryoo received the B.S., M.S., and Ph.D. degrees in electrical engineering from SungKyunkwan University, Seoul, Korea in 1991, 1995, and 2001, respectively. From 2004 to 2005, he was with WEMPEC at the University of Wisconsin-Madison, as a Visiting Scholar for his postdoctoral study. Since 1996, he has been with the Korea Electrotechnology Research Institute in Changwon, Korea. He is currently a Principal Research Engineer in the Electric Propulsion Research Division and a Leader of the Pulsed Power World Class Laboratory at that institute. Also, he has been a Professor in the Department of Energy Conversion Technology, University of Science & Technology, Deajeon, Korea, since 2005. His current research interests include pulsed power systems and their applications, as well as high power and high voltage conversions. He has published numerous papers at IEEE transactions and has obtained more than 20 Korean and industrial patents. Also he made 8 contracts with industrial firm based on his patents and succeeded to commercialize his high voltage solid state modulators. He received many awards due to industry applied technical contribution including ISTK Chairman Award from Korea Research Council for Industrial Science & Technology in 2009, Technical Award from Ministry of Science and Technology of Korea in 2010 and Dasan Technology Award from The Korea Economic Daily in 2011.

Dr. Ryoo is a member of the Korean Institute of Power Electronics (KIPE), and the Korean Institute of Electrical Engineers (KIEE).

Duk-Heon Kim was born in Daegu, Korea, in 1964. He received the B.S., M.S., and Ph.D. degrees in electrical engineering from SungKyunkwan University in Seoul, Korea in 1990, 1992, and 2002, respectively. Since 1994, he has been an associate professor in the department of electric railway, college of catholic sangji, Korea. His research interests mainly focused on power system & applications. He is a member of the Korean Institute of Power Electronics (KIPE), and the Korean Institute of Electrical Engineers (KIEE).